JOURNAL OF CATALYSIS 134, 311–316 (1992)

Oxygen-Diffusion-Limited CO Formation on a Ni Surface

R. J. McCLELLAND AND J. M. BLAKELY

Department of Materials Science and Engineering, Cornell University, Ithaca, New York 14853

Received February 8, 1991; revised September 23, 1991

The reaction between oxygen and carbon on a nickel film supported by a sapphire substrate has been studied with temperature programmed desorption (TPD) and Auger electron spectroscopy (AES). Oxygen was dissolved into the nickel film from the gas phase during high-temperature oxidation and annealing. Carbon was subsequently deposited on the nickel surface from the thermal decomposition of ethylene. During TPD, the bulk oxygen diffused to the vacuum interface of the nickel film, reacted with surface carbon, and desorbed as CO. A set of CO TPD peaks obtained for increasing initial carbon coverages showed a common low-temperature leading edge. This common leading edge has been fitted to a model in which the rate-limiting step in the carbon–oxygen reaction is taken to be the diffusion of bulk oxygen to the nickel film's surface. An activation energy for oxygen diffusion in nickel of 80 kcal/mole has been obtained. Sequential carbon exposures and TPD flashes eventually resulted in bulk oxygen depletion; this manifested itself in the CO desorption spectra as a reduction in the area under the CO peak and a shift of the peak to higher temperatures.

1. INTRODUCTION

The degradation of catalysts during use is a severe problem in the chemical industry. One form of catalyst deterioration is caused by poisoning by undesired contamination or intermediate species buildup (*1–3*). Sulfur is an example of the former (*4*), while carbon deposition during Fischer–Tropsch synthesis reactions (coking) typifies the latter (*5, 6*). One way to regenerate nickel-based catalysts which have lost their efficacy because of coking is to expose them to a high-temperature oxygen or steam treatment. This removes the carbon deposit through its oxidation to form CO and CO_2. The present study was undertaken to explore the role that dissolved oxygen in a metallic catalyst might play in the removal of surface carbon during thermal treatments. This paper summarizes the results of temperature programmed desorption and AES experiments on a model catalyst consisting of a single-crystal nickel film supported by a sapphire substrate.

2. EXPERIMENTAL

The nickel/sapphire specimen was prepared from eight-pass zone refined INCO 270 grade nickel, and single-crystal sapphire (Al_2O_3) disks of $(10\bar{1}1)$ orientation. A thin section of a nickel rod was placed between opposing sapphire disks, and the assembly was annealed in a vacuum furnace above 1726 K, and then cooled slowly over a 24-h period. A cut through the nickel layer resulted in two sapphire disks each covered by a continuous, circular-shaped nickel film. After final cutting, two 1.4 cm × 1.0 cm × 0.1 cm specimens were obtained. The nickel film was then mechanically and chemically polished to produce a layer 25 μm thick. X-ray Laue back reflection showed that the nickel film was predominantly a single crystal (*7*), and had a surface orientation that can be described in the notation of Thapliyal and Blakely (*8*) as Ni(111) 16° $[\bar{1}\bar{1}2]$. That is, the film was a Ni(111) surface rotated 16° about the $[\bar{1}\bar{1}2]$ zone axis toward $(1\bar{1}0)$. In conventional Miller indices, the nickel surface was very close to (423). A slot was then

0021-9517/92 $3.00

cut in the sapphire substrate parallel to the plane of the nickel film, leaving enough sapphire to permit the specimen to be hung over a tantalum ribbon heater for TPD. A chromel–alumel thermocouple was spot welded to the top portion of the nickel film for temperature measurement during TPD.

The UHV system has been described in more detail elsewhere (*9, 10*). It consisted of an ion and titanium sublimation pumped vacuum chamber equipped with a single-pass cylindrical mirror analyzer (CMA) for AES, an argon sputter ion gun for specimen cleaning, an ion gauge for pressure measurement, leak valves for gas admission, and a differentially pumped UTI 100C quadrupole mass spectrometer (QMS) with a line-of-sight detection tube for TPD. Since the area of the nickel film was greater than that of the TPD detection tube (~0.4 cm^2), and the specimen was positioned 1 mm from the tube during TPD, potential boundary effects from the nickel–sapphire interface and detection of desorption species from other parts of the vacuum chamber were avoided.

The specimen heating rate during TPD was ~14 K/s in the CO desorption temperature range. The QMS output for CO (m/e = 28) and the thermocouple voltage were recorded on a Hewlett Packard model 7004B x–y recorder. The recorded TPD spectra were transferred to a mainframe computer by use of an electronic digitizing tablet.

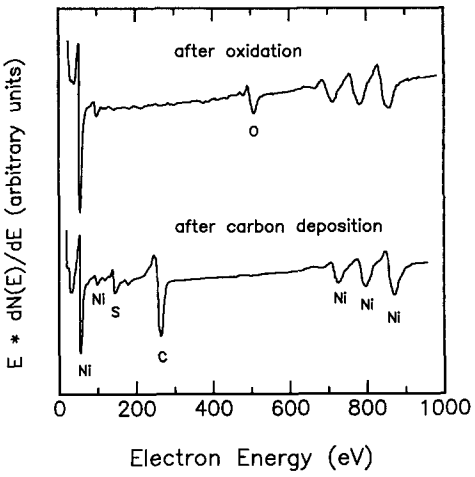

FIG. 1. AES spectra from the nickel film after different specimen treatments. The top spectrum is after oxidation at 773 K, and the bottom spectrum is after sputtering, annealing, and carbon deposition. The carbon coverage in this case is estimated to be ~2 Å, and appears to be of a graphitic nature (see text).

3. RESULTS AND DISCUSSION

Preliminary TPD experiments showed that the sapphire substrate did not appear to supply oxygen for reaction with surface carbon on the nickel film. After UHV anneals of the nickel/sapphire specimen at temperatures of 1073 K for several hours, followed by carbon deposition from the decomposition of ethylene (C_2H_4), no desorption species were measured by the QMS. The nickel film was then charged with oxygen by heating the specimen to 773 K and exposing to 1×10^{-6} Torr of oxygen for several hours. At the end of the oxidation, the sample was heated to 1173 K for several minutes until vacuum chamber wall desorption became excessive. The top AES spectrum in Fig. 1 shows the specimen surface after the oxidation procedure. The surface oxide was removed by argon ion sputtering at room temperature, and the specimen was then annealed at 813 K for 90 min prior to carbon deposition. No oxygen was detected by AES on the nickel surface after this treatment.

A carbon deposit was then formed on the specimen by heating to 643 K and exposing to 1×10^{-6} Torr of ethylene (C_2H_4) for various times to produce the desired quantity of carbon. The temperature for ethylene exposure was determined by concern over the fact that ethylene and CO would both have principal desorption peaks at m/e = 28. TPD spectra taken after room temperature ethylene exposure showed that there was almost no m/e = 28 desorption above 643 K. Stroscio *et al.* (*11*) had shown that ethylene was completely decomposed to atomic carbon by 500 K on Ni(110), and so it was felt that the contribution to the m/e = 28 peak during TPD after the high-temperature

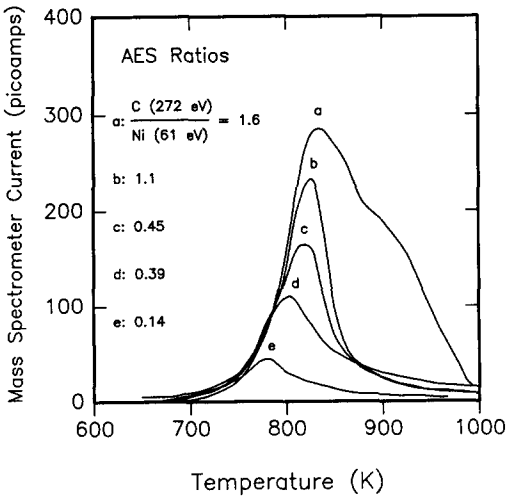

FIG. 2. CO (m/e = 28) desorption spectra from the specimen with various initial coverages of carbon. The AES ratios are based on peak-to-peak heights. TPD heating rate = 14 K/s.

carbon deposition procedure was caused by CO, and not ethylene. A final indication that the species recorded during TPD in this study was actually CO was the observation of m/e = 16 (oxygen) and m/e = 12 (carbon) peaks in experiments where those species were specifically monitored, consistent with the cracking pattern for CO. The bottom AES spectrum in Fig. 1 shows the nickel surface after a typical amount of carbon was deposited. The carbon coverage for this particular surface preparation was estimated to be ~2 Å, based on the attenuation of the Ni 61-eV Auger peak after carbon deposition (*12*) and the estimated inelastic mean free path and attenuation length for 61 eV electrons in carbon (*13, 14*). The deposited carbon overlayer showed Auger peak shapes characteristic of graphite (*15–17*). TPD was then performed after the carbon deposition step. The specimen was annealed at 1173 K for 1 min after the completion of a TPD flash to redistribute the dissolved oxygen prior to the carbon deposition step preceeding the next TPD flash. This annealing step was performed to replenish near-surface oxygen removed by the flash.

Figure 2 shows a series of CO TPD spectra taken from the nickel/sapphire specimen for increasing amounts of carbon coverage. The relative carbon coverage is expressed as the ratio of the carbon 272-eV AES peak to the nickel 61-eV peak. The significant feature is the common low-temperature leading edge of the CO desorption peak exhibited by the family of TPD spectra, indicating that the initial rate of CO desorption is independent of the carbon concentration on the surface. List and Blakely (*18*) have previously observed very similar behavior for a set of CO TPD spectra from oxygen-exposed nickel crystals which contained dissolved carbon. However, the lower temperature β_1 CO desorption peak (*18*) was not observed in the present experiment; this peak was believed to be caused by the reaction between surface carbon and surface oxygen in the previous study and had been observed in the ~500–650 K temperature range. The absence of the β_1 CO desorption peak in this study is consistent with the lack of oxygen on the nickel surface at the beginning of the TPD flash (as determined by AES). List and Blakely proposed that the rate-limiting step for the formation of the β_2 CO desorption peak (the label given the highest temperature CO desorption peak in their study) was the diffusion of bulk carbon to the surface of the nickel specimen, and derived an equation relating the CO desorption flux to the carbon diffusivity in nickel, the carbon concentration, and the heating rate used in the TPD experiments. The activation energy they obtained for C diffusion in nickel (E_d = 36.5 kcal/mole), and preexponential factor (D_0 = 0.04 cm^2/s), were in reasonable agreement with values measured by Diamond and Wert using anelastic techniques (*19*).

The present investigation is an analogous diffusion study, except that the initial distributions of carbon and oxygen are reversed: carbon is now the surface species, and oxygen is dissolved in a nickel film. If bulk oxygen diffusion to the surface is the rate-limiting step in the CO desorption spectra in Fig. 2, the same analysis should be applica-

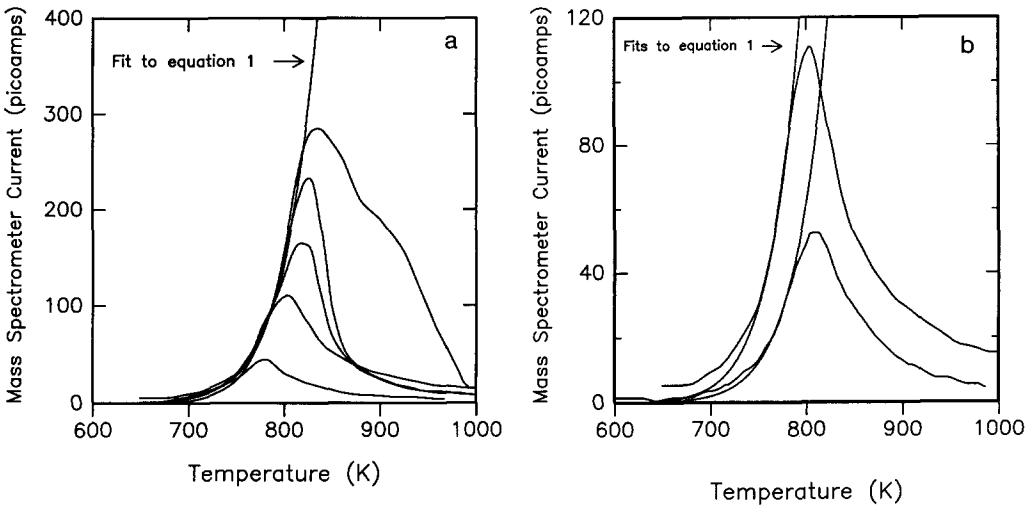

FIG. 3. (a) Least squares fit of Eq. (1) to the CO desorption peaks in Fig. 2 (b) Least squares fits of Eq. (1) to spectrum (d) of Fig. 2 and to a later flash when the specimen showed characteristics of oxygen depletion; that is, a displacement of the CO peak to a higher temperature. Both fits use the value of 80 kcal/mole for E_d.

ble, and the flux of oxygen to the vacuum interface of the nickel film during TPD would be given by (*18*)

$$J(T) = \frac{[(C_0^2 D_0 \beta)/\pi]^{0.5} \exp(-E_d/kT)}{\left[\int_{T_0}^{T} \exp(-E_d/kT')dT'\right]^{0.05}}, \quad (1)$$

where C_0 is the bulk oxygen concentration, β is the TPD heating rate, T is the specimen temperature, T_0 is the TPD-initiation temperature, and k is the Boltzmann constant. The oxygen diffusivity, D, has been taken to follow an Arrhenius form

$$D = D_0 \exp(-E_d/kT), \quad (2)$$

where D_0 is the oxygen diffusivity preexponential, and E_d is the activation energy for oxygen diffusion in nickel. The CO desorption flux would then be directly proportional to the flux of dissolved oxygen to the surface if oxygen diffusion were rate-limiting.

Equation (1) was fitted to the CO desorption spectra shown in Fig. 2 by arbitrarily selecting a value for $C_0^2 D_0$ that resulted in coincidence of Eq. (1) with the midpoint of the common leading edge of the family of TPD spectra, and varying E_d until a minimum in the sum of the squares of the difference between the fit and the common leading edge was achieved. A value of 80 kcal/mole was then obtained for the activation energy for oxygen diffusion in nickel. This value is in fair agreement with other studies of oxygen diffusivity in nickel (using internal oxidation techniques) which reported values of 71–74 kcal/mole for E_d (*20–23*). Figure 3a shows the fit of the bulk-oxygen-diffusion-limited model superimposed on the data of Fig. 2. It should be noted that Eq. (1) predicts an exponentially increasing flux of oxygen to the nickel surface, but actual experiments must eventually deviate from this because one or both of the reactants will become depleted during the TPD flash: in the present case carbon on the surface is believed to be completely consumed during the flash, causing a peak in the CO desorption spectrum.

Figure 3b shows the CO TPD spectrum of curve (d) in Fig. 2 and that from a later flash. One can see that the CO desorption peaks for these two flashes did not exhibit the common low-temperature leading edge behavior

seen earlier. In this case, after a new carbon adlayer was deposited, a third TPD flash showed no CO desorption. It is believed that the shift of the CO TPD peak to higher temperatures was caused by the depletion of bulk oxygen from the limited volume of the nickel film. It was generally observed that if a series of experiments was continued beyond approximately four TPD flashes, subsequent CO desorption peaks shifted to increasingly higher temperatures, with each peak reduced in magnitude, until a point at which no CO was desorbed during TPD.

List (*10*) was able to determine values for the quantities D_0 and C_0 for carbon diffusion in nickel by fitting Eq. (1) (after a value for E_d was obtained) to a series of TPD spectra from specimens which were not annealed between flashes. For the unannealed cases, the CO desorption spectra progressively shifted to higher temperatures during a series of flashes because the bulk carbon concentration near the surface was no longer the constant value assumed in the model. His technique for extracting D_0 and C_0 relied on a uniform, but incremental, decrease in the nickel specimen's near-surface carbon concentration, a decrease which is caused by the removal of carbon as CO during the TPD flash, and not compensated for by a post-TPD high-temperature anneal. In the present study, if the specimen was not annealed between TPD flashes to redistribute dissolved oxygen, the removal of near-surface oxygen during TPD should cause a progressive shift of the CO peaks to higher temperatures. Theoretically, this shift would permit the use of List's technique for calculating D_0 and C_0. Unfortunately, D_0 and C_0 for oxygen diffusion in nickel could not be separately extracted because the dissolved oxygen was completely depleted almost immediately after the TPD spectra began to shift to higher temperatures (see Fig. 3b), leaving an insufficient number of TPD spectra exhibiting oxygen depletion for quantitative analysis.

If the specimen was reoxidized, high-temperature annealed to dissolve oxygen, sputter cleaned to remove surface oxygen, then low-temperature annealed to remove sputter damage, CO TPD spectra which had coincident low temperature leading edges with the data of Fig. 2 could be regenerated after the carbon deposition step. Figure 4 shows AES results prior to and after a TPD flash which showed no CO desorption. The carbon layer was gone after the flash, presumably through dissolution into the nickel film. Situations in which surface carbon dissolution occurs concurrently with the oxidation reaction complicates the proposed model; however, quantitative measurements for the activation energy for oxygen diffusion in nickel were only made for cases in which it appeared that all surface carbon participated in the oxidation reaction, and subsequently desorbed as CO.

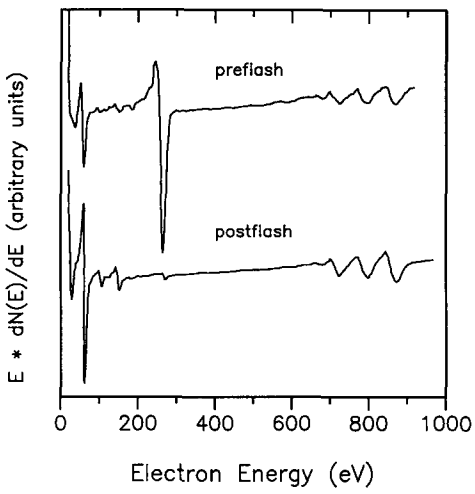

FIG. 4. AES spectra from the nickel surface before and after a TPD flash to 1000 K in which no CO was desorbed. The drastic reduction of the carbon signal after the flash is caused by carbon dissolution into the crystal.

Figure 3b also illustrates the fit of Eq. (1) (with the same activation energy for oxygen diffusion in nickel, E_d = 80 kcal/mole, as derived from Fig. 2) superimposed on the CO spectrum which was shifted to higher temperatures, but with a smaller value chosen for the $C_0^2 D_0$ term. The oxygen-diffusion-limited CO desorption model is consis-

tent with the experimental observations even when oxygen depletion is believed to occur, and can be accounted for in the model by a reduction in the C_0^2 term. The model should, however, be applied carefully since there may be systems in which the rate-limiting step is not simply the diffusion of oxygen to the surface, but, instead, some other process, such as the surface recombination reaction itself.

4. SUMMARY

TPD and AES experiments on a nickel film supported by a sapphire substrate demonstrated that oxygen, which was dissolved in the nickel film, was able to diffuse to the nickel surface and react with surface carbon during specimen heating to form CO; the CO subsequently desorbed from the nickel surface. A series of CO desorption spectra for various initial carbon coverages consisted of a set of peaks, which had a common low-temperature leading edge. The CO desorption rate is consistent with a model in which the rate-limiting step is the diffusion of bulk oxygen to the surface of the nickel film, and a value of 80 kcal/mole was calculated for the activation energy for oxygen diffusion in nickel. Continued carbon exposure and TPD flashes caused bulk oxygen depletion of the nickel film, resulting in a shift to higher temperatures of the CO desorption peak; eventually no CO desorption was observed. The bulk oxygen concentration could be restored by high-temperature oxidation and annealing, and CO TPD spectra from the specimen after this treatment again showed a common low-temperature leading edge.

ACKNOWLEDGMENTS

The authors thank B. F. Addis for his skillful preparation of the specimen and Margaret Rich for her careful X-ray Laue examination. Fred List is gratefully acknowledged by RJM for valuable discussions and experimental assistance early in this study. This work was supported by the National Science Foundation, Grant DMR-8820362, and by the Cornell Materials Science Center through the use of its facilities.

REFERENCES

1. Hegedus, L., and McCabe, R. W., "Catalyst Poisoning." Dekker, New York, 1984.
2. Hughes, R., "Deactivation of Catalysts." Academic Press, New York, 1984.
3. Oudar, J., and Wise, H. (eds.), "Deactivation and Poisoning of Catalysts." Dekker, New York, 1985.
4. Somorjai, G. A., *J. Catal.* **27,** 453 (1972).
5. Bartholomew, C. H., *Catal. Rev. Sci. Eng.* **24,** 67 (1982).
6. Wigmans, T., Van Doorn, J., and Moulijn, J. A., *Surf. Sci.* **135,** 532 (1983).
7. McClelland, R. J., M.S. Thesis, Cornell Univ., Ithaca, NY (1987); Cornell Materials Science Center Report 7117 (1987).
8. Thapliyal, H. V., and Blakely, J. M., *J. Vac. Sci. Technol.* **15,** 600 (1978).
9. List, F. A., and Blakely, J. M., *J. Vac. Sci. Technol.* **20,** 838 (1982).
10. List, F. A., PhD Thesis, Cornell Univ., Ithaca, NY, 1982; Cornell Materials Science Center Report 4791 (1982).
11. Stroscio, J. A., Bare, S. R., and Ho, W., *Surf. Sci.* **148,** 499 (1984).
12. Eizenberg, M., and Blakely, J. M., *Surf. Sci.* **82,** 228 (1979).
13. Lesiak, B., Jablonski, A., Prussak, Z., and Mrozek, P., *Surf. Sci.* **223,** 213 (1989).
14. Tanuma, S., Powell, C. J., and Penn, D. R., *Surf. Sci.* **192,** L849 (1987).
15. Coad, J. P., and Riviere, J. C., *Surf. Sci.* **25,** 609 (1971).
16. Patil, H. R., and Blakely, J. M., *J. Appl. Phys.* **45,** 3806 (1974).
17. Goodman, D. W., Kelley, R. D., Madey, T. E., and Yates, J. T., Jr., *J. Catal.* **63,** 226 (1980).
18. List, F. A., and Blakely, J. M., *Surf. Sci.* **152/153,** 463 (1985).
19. Diamond, S., and Wert, C., *Trans. Metall. Soc. AIME* **239,** 705 (1967).
20. Barlow, R., and Grundy, P. J., *J. Mater. Sci.* **4,** 797 (1969).
21. Goto, S., Nomaki, K., and Koda, S., *J. Jpn. Inst. Met.* **31,** 600 (1967). [Abstracted by *Diffusion Data* **1,** 39 (1967).]
22. Lloyd, G. J., and Martin, J. W., *Met. Sci. J.* **7,** 7 (1973).
23. Louthan, M. R. Jr., and Dexter, A. H., *Met. Sci. J.* **7,** 76 (1973).